THE JOURNAL OF PHYSICAL CHEMISTRY B

Article

pubs.acs.org/JPCB

Modeling Ring/Chain Equilibrium in Nanoconfined Sulfur

Fatema Begum,[†] Rakibul H. Sarker,[‡] and Sindee L. Simon*,[†]

[†]Department of Chemical Engineering, Texas Tech University, Lubbock, Texas 79409-3121, United States

[‡]Department of Petroleum Engineering, Marietta College, Marietta, Ohio 45750, United States

ABSTRACT: The effect of nanoconfinement on the thermodynamics of free radical polymerization of sulfur is examined. We extend Tobolsky and Eisenberg's model of bulk sulfur polymerization to nanopores accounting for the confinement entropy of the chains and ring using scaling reported in literature. The model quantitatively captures literature data from Yannopoulos and co-workers for the extent of polymerization versus temperature for bulk sulfur polymerization and for polymerization in 20, 7.5, and 2.5 nm diameter Gelsil nanopores, assuming that the change of entropy of nanoconfined chains scales with molecular size to the second power and with nanopore diameter to either the −3.0 or −3.8 power, the former of which fits slightly better. The scaling, which is valid for strong confinement in spherical pores, predicts that the propagation equilibrium constant will depend on both nanopore size and chain length, such that the average chain length decreases significantly upon confinement.

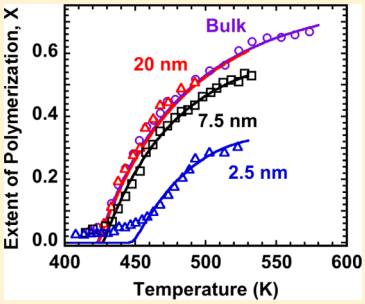

INTRODUCTION

Nanoscale confinement has an impact on the properties of small molecules and polymeric materials, including the melting point,[1] glass transition temperature (T_g),[1] modulus,[2−4] thermal expansion coefficient,[5−7] and reactivity and reaction rates.[8−16] In addition, polymerization of substituted alkenes under nanoconfinement influences the molecular weight,[17−25] polydispersity index (PDI),[17−21,24] and degree of tacticity[21] of the resulting polymer. In the case of sulfur, which shows a floor polymerization temperature, the equilibrium between eight-membered rings and linear chains is shifted to higher temperatures in nanoporous Gelsil monolithic silica matrices (from GelTech, Inc.), and the limiting conversion also decreases with decreasing confinement size.[26,27]

Our objective is to model the effects of nanoconfinement on sulfur polymerization by extending Tobolsky and Eisenberg's model.[28] We do this by accounting for the confinement entropy of chains using the scaling in the literature:[29−32]

$$\Delta S_{conf} \propto -N^{p}D^{-m} \tag{1}$$

where ΔS_{conf} is the change of entropy of a confined chain, N is the number of bonds in the chain, and D is the nanopore diameter. The exponent p is equal to either 1.0 or 2.0 according to scaling in a weak or strong confinement.[29,30] The exponent m for the pore diameter has been suggested to be 1.7 for cylindrical confinement,[29,30] 3.0 for spherical confinement based on self-consistent field theory,[31] or 3.8 or 3.9 for spherical confinement using blob theory in semidilute solutions.[32] As will be shown, the implication of our model is that the sulfur ring/chain equilibrium constant in nanopores will depend on chain length, as well as pore size; this differs from the explanation provided by Kalampounias and co-workers,[26] who interpreted their data for Gelsil nanoconfined sulfur also assuming that the ring/chain equilibrium constant decreases under confinement but that the values only depend on pore size and not on chain size.

The paper is organized as follows. We first present the Tobolsky and Eisenberg model of equilibrium living polymerization of bulk unconfined sulfur, along with the changes to capture the reaction in nanopores. A brief methodology section follows, and then we compare modeling results with experimental data from the literature[26,27] and discuss the implications.

Polymerization Model. The kinetic model of living sulfur polymerization described Tobolsky and Eisenberg[28] involves several elementary steps. The first step of the reaction is initiation, in which an eight-membered S_8 ring (M) forms an S_8^* radical (M_1^*):

$$M \overset{K_1}{\rightleftharpoons} M_1^* \tag{2}$$

where K_1 is the equilibrium constant for the initiation reaction. Subsequent steps involve propagation to form active radicals having n S_8 monomer units, M_n^*:

$$M + M_{n-1}^* \overset{K_n}{\rightleftharpoons} M_n^* \tag{3}$$

where K_n is the equilibrium constant for the nth reaction. The concentration of free radical species, M_n^* can be expressed in term of the equilibrium constants and the equilibrium concentration of monomer M:[28]

$$M_1^* = K_1 M \tag{4}$$

$$M_2^* = K_2 M M_1^* = K_1 K_2 M^2 \tag{5}$$

Received: January 5, 2013
Revised: March 9, 2013
Published: March 11, 2013

   dx.doi.org/10.1021/jp400145n | J. Phys. Chem. B 2013, 117, 3911−3916

$$M_n^* = K_n M M_{n-1}^* = K_1 K_2 K_3 \ldots\ldots K_n M^n = K_1 \left(\prod_{i=2}^{n} K_i\right) M^n \tag{6}$$

Following the work of Tobolsky and Eisenberg,[28] K_n is independent of n for $n > 1$, such that

$$M_n^* = K_1 K^{n-1} M^n \tag{7}$$

where K is the equilibrium constant for propagation. After algebraic rearrangement and simplification of the binomial series expansions, the total concentration of polymer P, the number average degree of polymerization x_n, and conversion X are given by the following expressions:[28]

$$P = \sum M_n^* = \frac{K_1 M}{1 - KM} \tag{8}$$

$$x_n = \frac{\sum n M_n^*}{\sum M_n^*} = \frac{1}{1 - KM} \tag{9}$$

$$X = \frac{M_o - M}{M_o} = \frac{P x_n}{M_o} = \frac{K_1 M}{M_o (1 - KM)^2} = \frac{K_1 M_o (1 - X)}{M_o [1 - K M_o (1 - X)]^2} \tag{10}$$

where M_o is the initial monomer concentration of S_8 rings. Equation 10 can be solved analytically to obtain the value of the conversion X and, thus, the equilibrium monomer concentration M as a function of temperature, the latter of which can then be used to obtain the P and x_n from eqs 8 and 9.

The equilibrium constants K_1 and K are functions of temperature and can be expressed in terms of the standard change in Gibbs free energy on reaction.[33] For the propagation step,

$$K = \exp[-\Delta G / RT] \tag{11}$$

where the standard change in Gibbs free energy at temperature T, ΔG is given by

$$\Delta G = \Delta H_o - T \Delta S_o + \Delta C_p [(T - T_o) - T \ln(T/T_o)] \tag{12}$$

and ΔH_o and ΔS_o are the standard change in enthalpy and entropy for the propagation reaction at T_o, respectively, ΔC_p is the change in heat capacity for the propagation reaction, and T_o is the reference temperature. Assuming that ΔC_p is zero for the initiation reaction, the rate constant K_1 is simply given by

$$K_1 = \exp[-\Delta H_1 / RT] \exp[\Delta S_1 / R] \tag{13}$$

where ΔH_1 and ΔS_1 are the standard change of enthalpy and entropy of initiation, respectively, and are assumed to be independent of temperature.

In order to extend the model to the case of nanoconfinement, we must consider the change in entropy on confinement and how that will influence initiation and propagation rate constants. For the initiation step, both the S_8 ring reactant and the S_8^* radical are small and of similar size, and hence, we assume that the entropy of initiation and K_1 are not influenced by nanoconfinement. For the propagation reaction on the other hand, we go from a chain of size n and an S_8 ring to a chain of size $n + 1$. For the case of weak confinement,[29,30] the change in entropy of propagation due to confinement effects is expected to be zero, being proportional to $[(n + 1) - n - 1]$ since confinement entropy is proportional to chain length to the first power (N^1); thus, for weak confinement, the propagation equilibrium constant K will not be influenced by confinement. However, in the case of strong confinement, confinement entropy is thought to scale with the square of the chain size: $\Delta S_{conf} \propto N^2$. The entropy change on propagation is, thus, expected to be modified as follows for the nth propagation reaction:

$$\Delta S_n = \Delta S_{o,bulk} + \Delta C_p \ln \frac{T}{T_o} - c[(n+1)^2 - n^2 - 1] D^{-m} = \Delta S_{o,bulk} + \Delta C_p \ln \frac{T}{T_o} - 2cnD^{-m} \tag{14}$$

where $\Delta S_{o,bulk}$ is the standard change in entropy for propagation in the bulk at T_o (=ΔS_o in eq 12 for the bulk case), n is the chain length in terms of S_8 units, and c is a prefactor. Hence, in the case of strong confinement, the simplifying assumption that $K_n = K$ is no longer valid. Rather, K_n is expected to decrease with increasing chain length and is given by the following expression assuming that the enthalpy of reaction is unaffected by confinement, the latter of which is found to be the case for free radical and step polymerizations studied in our laboratory:[10−12,14]

$$K_n = \exp\left[-\frac{\Delta H_o}{RT} + \frac{\Delta S_{o,bulk}}{R} - \frac{\Delta C_p}{RT}\left(T - T_o - T \ln \frac{T}{T_o}\right) - \frac{2cnD^{-m}}{R}\right] \tag{15}$$

The following equations for total concentration of polymer P, number average degree of polymerization x_n, and conversion X can then be simultaneously solved at a given temperature:

$$P = \sum M_n^* = \sum_{n=1}^{\infty} K_1 \left(\prod_{i=2}^{n} K_i\right) M^n \tag{16}$$

$$x_n = \frac{\sum n M_n^*}{P} = \frac{1}{P} \sum_{n=1}^{\infty} K_1 \left(\prod_{i=2}^{n} K_i\right) n M^n \tag{17}$$

$$X = \frac{M - M_o}{M_o} = \frac{P x_n}{M_o} \tag{18}$$

Methodology. In the present work, a computer code written in MATLAB is used to perform the numerical calculations to obtain P, x_n, and X as a function of temperature (T) by solving eqs 16−18 with eqs 11−13 defining equilibrium constants in the bulk case, and eqs 13 and 15 defining the equilibrium constants in the nanoconfinement case. A numerical method is implemented to search for the correct equilibrium value of M at a particular temperature. The correct value of M should equal the difference between M_o and the amount of monomer in polymer ($P x_n$); we find this value specifying that the error $\varepsilon = M_o - P x_n - M < 1 \times 10^{-6}$ mol/kg.

The numerical solution for the bulk unconfined case should equal the analytical calculation given by eqs 8−10, and this has been verified to be the case as shown in Figure 1. The values of the parameters used in the model calculations are given in Table 1, with parameters taken from the literature for the bulk unconfined polymerization[26] for M_o, ΔH_1, ΔS_1, ΔH_o, and $\Delta S_{o,bulk}$ (=ΔS_o in eq 12 for the bulk case). As shown in Figure 1, the extent of reaction goes to unity at high temperatures

dx.doi.org/10.1021/jp400145n | J. Phys. Chem. B 2013, 117, 3911−3916

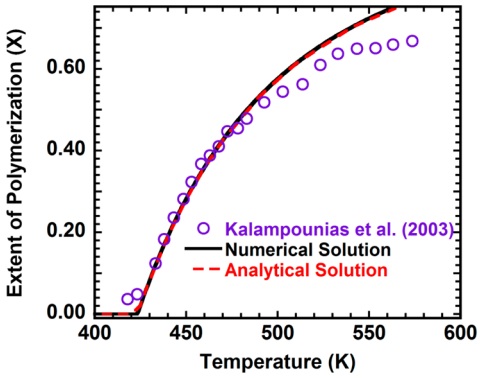

Figure 1. Model predictions for the extent of polymerization versus temperature for sulfur polymerization in the bulk assuming $\Delta C_p = 0$. Comparison of the numerical and analytical solutions and experimental data from ref 26 using model parameters from ref 26.

Table 1. Values of Model Parameters

parameter	expression or values	references
M_o (mol/kg)	3.9	26
ΔH_1 (kJ/mol)	117.15	26
ΔS_1 (J/mol/K)	13.39	26
ΔH_o (kJ/mol)	19.66	26
$S_{o,bulk}$ (J/mol/K)	35.15	26
T_o (K)	423.15	
ΔC_p(J/mol/K)	−62.84 (bulk and 20 nm)	present work
	−113.21 (7.5 nm)	
	−163.44 (2.5 nm)	
c (nm^{3}J/mol/K)	0.15 (for m = 3.0)	present work
	0.30 (for m = 3.8)	

when ΔC_p is taken to be zero. To capture the experimentally observed[26,27] limiting conversions, which are below unity, ΔC_p for the propagation reaction must be negative, implying that the propagation reaction product of length n has less degrees of freedom than the monomer and chain of length $n - 1$.

The parameters ΔC_p and c are obtained by fitting the model to the experimental data assuming the literature values reported for bulk polymerization are valid at the reference temperature of T_o = 150 °C (423 K, which is very near the floor temperature for bulk sulfur; see Table 2). We assume that the scaling exponent for chain length p equals 2.0, and that for the pore diameter m equals either 3.0 or 3.8 (see eq 1). The choice of m = 3.0 is expected for spherical confinement for self-consistent

Table 2. Experimental and Predicted Transition Temperatures

pore size (nm)	transition peak temperature (°C)[b]	transition breadth (°C)[b]	transition onset (°C)[b]	predicted onset (°C)[a] m = 3.0	predicted onset (°C)[a] m = 3.8
bulk	434	14	427	427	428
20	434	14	427	428	428
7.5	452	36	434	432	430
2.5	478	44	456	455	455

[a]The predicted onset is the temperatures at which model calculations predict 5% conversion will be reached. [b]The transition peak temperature and breadth are from ref 27; the onset is then determined from the peak temperature minus half of the transition breadth.

field theory,[31] and this is the type of confinement that is thought to be provided by Gelsil glasses,[34,35] whereas the value of m = 3.8 is for spherical confinement according to blob theory.[32] The use of m = 1.7, for cylindrical confinement,[29,30] was also attempted and will be discussed.

RESULTS

A comparison of the extent of polymerization X versus polymerization temperature calculated in the present work with the experimental Raman spectroscopy data from Yannopoulos and co-workers[27] is shown in Figure 2 for sulfur

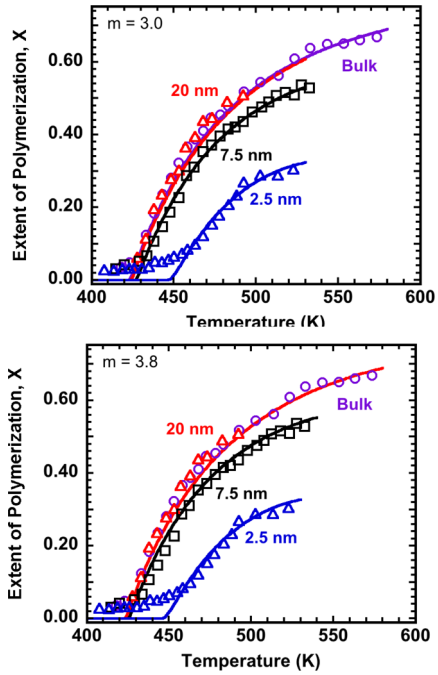

Figure 2. Model predictions (solid lines) and experimental data (open symbols)[27] for the extent of polymerization versus temperature for sulfur polymerization in bulk and in 20, 7.5, and 2.5 nm pores for m = 3.0 (upper panel) and m = 3.8 (lower panel). Parameters used for the calculations are given in Table 1.

in the bulk unconfined state and in 20, 7.5, and 2.5 nm pores of Gelsil glass. Calculations shown in the upper panel of Figure 2 use a scaling exponent for pore diameter of m = 3.0, whereas calculations shown in the lower panel use an exponent of 3.8. Good agreement is obtained between the present work and the experimental data for both exponents, although the exponent of 3.0 gives a slightly better fit. For the bulk, the conversion increases rapidly at approximately 430 K with increasing temperature, leveling off at approximately 67% conversion at 573 K. The data in 20 nm diameter pores is indistinguishable from the bulk within the error of the measurements. For the two smallest pore sizes, the transition temperature is shifted to higher temperatures with decreasing pore size, and the limiting conversion at high temperatures decreases. Our model captures both of these results with two fitting parameters, c and ΔC_p, for both m = 3.0 and 3.8. On the other hand, for planar or cylindrical confinement[29,30] where m is equal to 1.7, the dependence on D is weaker, and the model cannot adequately capture the pore size dependence; i.e., with m = 1.7, the model predicts that the data for 2.5 and 20 nm-diameter pores should be closer to one another than experimentally observed. Hence,

dx.doi.org/10.1021/jp400145n | J. Phys. Chem. B 2013, 117, 3911−3916

although theoretically one might expect a model assuming a fraction of spherical pores (m = 3.0) connected by a fraction of cylindrical pores (m = 1.7) might give an improved fit, this is not the case for this data.

A quantitative comparison between the floor temperature observed experimentally and that predicted by the model is shown in Table 2, where the experimental values are based on transition peak temperatures and breadths reported in the literature,[27] and model predictions are taken to be the temperature at which 5% conversion is reached. Although good agreement between the model and experimental values is observed, consistent with the fits shown in Figure 2, the model does not capture the "rounding" of the transition and increase in transition breadth that is experimentally observed[26,27] for the smallest pore sizes. The rounding of the transition, which can be clearly seen in Figure 2 for the 2.5 nm data, is attributed to finite size effects.[26] A similar finite size effect has been observed and modeled in cell-surface receptor aggregates using a kinetic Monte Carlo model,[36] but we did not attempt to capture this effect here.

As already mentioned, in order to capture a limiting conversion below unity, ΔC_p must be negative, and furthermore, the value must decrease (become more negative) with decreasing pore size to capture the fact that the limiting conversion decreases with decreasing pore size. For the bulk, a value of ΔC_p of −0.245 J/g/K or −62.8 J/mol/K (per mole of the S_8 ring) well describes the data, and this is consistent with the literature value of −0.163 J/g/K.[37] For smaller pore sizes, ΔC_p appears to be a larger, more negative, number; however, there is no data in the literature to compare this with, and future experiments are planned to test this prediction from the model. The implication is that more degrees of freedom are lost on propagation in a nanopore than in the bulk.

DISCUSSION

The experimental data for nanoconfined polymerization of sulfur in the bulk and in Gelsil nanopores[26,27] is well explained by extension of the Tobolsky and Eisenberg model in which the propagation equilibrium rate constant K_n is assumed to be a function of temperature, as well as a function of chain length and confinement size consistent with $\Delta S_{conf} \propto -N^2 D^{-m}$, where m is either 3.0 or 3.8, with the exponent 3.0 giving a slightly better fit. The values of K_n at 473 K are plotted as a function of chain length n in Figure 3 with the solid lines indicating the results for our model for m = 3.0 and dashed lines indicating the results for m = 3.8. The value of K_n is constant for the bulk, in accordance with the Tobolsky and Eisenburg assumption, but it decreases with increasing chain length in nanoconfinement. On the other hand, the dotted lines in Figure 3 for the bulk and for nanoconfinement in 2.5 nm diameter pores show the values obtained by Yannopoulos and co-workers,[26] assuming that the propagation equilibrium constant is only a function of confinement size and is independent of n.

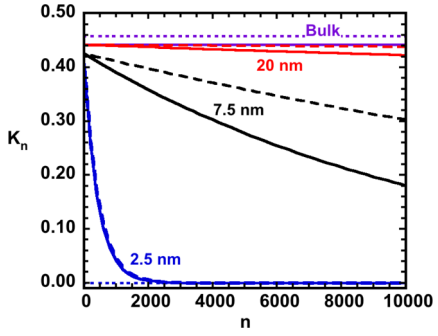

Figure 3. Model predictions for the propagation equilibrium rate constant K_n as a function of chain length n at 473 K for sulfur polymerization in bulk and in 20, 7.5, and 2.5 nm-diameter pores for m = 3.0 (solid lines) and m = 3.8 (dashed lines). Dotted lines shown for the bulk and for nanoconfinement in 2.5 nm diameter pores reflect values obtained by Yannopoulos and co-workers.[26]

In order to demonstrate the effect of nanoconfinement on the number average degree of polymerization x_n, Figure 4 shows our model predictions for x_n as a function of temperature for bulk polymerization and polymerization in 20, 7.5, and 2.5 nm pores. The change of x_n with temperature is gradual initially and then shows a sharp increase at approximately 423 K except in the smallest pores where the increase in chain length with temperature is more gradual. The maximum value of x_n decreases with decreasing pore size, and at 473 K, the number average degree of polymerization x_n for the bulk is 30 000. In nanoporous confinement, x_n decreases quite dramatically to 2400, 600, and 125 for 20, 7.5, and 2.5 nm diameter pores, respectively, for m = 3.0. Values are slightly higher for 20 and 7.5 nm pores for m = 3.8. Even in 20 nm diameter pores, where the extent of polymerization is seemingly unaffected by nanoconfinement, as shown in Figure 2, chain length decreases 2 orders of magnitude compared to the bulk because of the dependence of K_n on chain length.

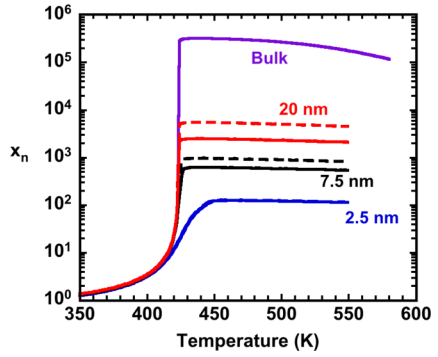

Figure 4. Model predictions for the number average degree of polymerization (x_n) versus temperature for sulfur polymerization in bulk and in 20, 7.5, and 2.5 nm-diameter pores for m = 3.0 (solid lines) and m = 3.8 (dashed lines); the two lines are indistinguishable for 2.5 nm-diameter pores.

Based on our calculation, the maximum value of number average degree of polymerization for the smallest pore size is 125 at 473 K. On the other hand, for the same 2.5 nm-diameter pore size, Kalampounias et al.[26] estimated that the maximum value would be 3.2×10^4 assuming that the propagation equilibrium constant was a constant value of 2.1×10^{-13} at 473 K. Determination of the degree of polymerization under nanoconfinement is needed to differentiate our model, which assumes a chain length-dependent K_n, from the model of Yannopoulos and co-workers, which does not; such measurements have not been made. We argue, however, that if confinement entropy is the origin of the shift in ring/chain equilibrium, then the equilibrium should depend on the size of the chain relative to that of confinement resulting in a chain size-dependent equilibrium constant. The result is anticipated to be relevant for all nanoconfined equilibrium reactions and

dx.doi.org/10.1021/jp400145n | J. Phys. Chem. B 2013, 117, 3911−3916

may well be relevant to equilibrium reactions in crowded environments, such as protein dimerization in cells.

CONCLUSIONS

The ring/chain equilibrium model for sulfur is extended for polymerization in nanopores assuming that the equilibrium propagation constant depends on both confinement size and chain length. Scaling from the literature is applied for the regime of strong, spherical porous confinement, in which the change of entropy of confined chains scales with molecular size to the second power and with nanopore diameter to either the −3.0 or −3.8 powers, the latter giving a somewhat better fit. In both bulk and nanopore-confined cases, the model well describes the experimental data of Yannopoulos and co-workers[26,27] which shows that the transition temperature shifts to higher temperatures with nanoconfinement in Gelsil pores and the limiting conversion correspondingly decreases. The maximum value of number average degree of polymerization is also predicted to decrease significantly with decreasing pore size. The model differs from previous models in the assumption that the equilibrium constant depends on chain size relative to pore size, and this assumption has important implications for understanding nanoconfined equilibrium reactions.

AUTHOR INFORMATION

Corresponding Author

*E-mail: sindee.simon@ttu.edu.

Notes

The authors declare no competing financial interest.

ACKNOWLEDGMENTS

Funding from the American Chemical Society Petroleum Research Fund 52426-ND7 is gratefully acknowledged.

REFERENCES

(1) Alcoutlabi, M.; McKenna, G. B. Effects of Confinement on Material Behaviour at the Nanometre Size Scale. *J. Phys.: Condens. Matter* **2005**, *17*, R461−R524.

(2) Domke, J.; Radmacher, M. Measuring the Elastic Properties of Thin Polymer Films with the Atomic Force Microscope. *Langmuir* **1998**, *14*, 3320−3325.

(3) Du, B. Y.; Tsui, O. K. C.; Zhang, Q. L.; He, T. B. Study of Elastic Modulus and Yield Strength of Polymer Thin Films Using Atomic Force Microscopy. *Langmuir* **2001**, *17*, 3286−3291.

(4) Stafford, C. M.; Vogt, B. D.; Harrison, C.; Julthongpiput, D.; Huang, R. Elastic Moduli of Ultrathin Amorphous Polymer Films. *Macromolecules* **2006**, *39*, 5095−5099.

(5) Lenhart, J. L.; Wu, W. L. Deviations in the Thermal Properties of Ultrathin Polymer Network Films. *Macromolecules* **2002**, *35*, 5145−5152.

(6) Pochan, D. J.; Lin, E. K.; Satija, S. K.; Wu, W. L. Thermal Expansion of Supported Thin Polymer Films: A Direct Comparison of Free Surface vs Total Confinement. *Macromolecules* **2001**, *34*, 3041−3045.

(7) Soles, C. L.; Douglas, J. F.; Wu, W. L.; Peng, H. G.; Gidley, D. W. Comparative Specular X-ray Reflectivity, Positron Annihilation Lifetime Spectroscopy, and Incoherent Neutron Scattering Measurements of the Dynamics in Thin Polycarbonate Films. *Macromolecules* **2004**, *37*, 2890−2900.

(8) Amanuel, S.; Malhotra, V. M. Effects of Physical Confinement (< 125 nm) on the Curing Behavior of Phenolic Resin. *J. Appl. Polym. Sci.* **2006**, *99*, 3183−3186.

(9) Li, Q. X.; Hutcheson, S. A.; McKenna, G. B.; Simon, S. L. Viscoelastic Properties and Residual Stresses in Polyhedral Oligomeric Silsesquioxane (POSS)-Reinforced Epoxy Matrices. *J. Polym. Sci., Part B: Polym. Phys.* **2008**, *46*, 2719−2732.

(10) Li, Q. X.; Simon, S. L. Surface Chemistry Effects on the Reactivity and Properties of Nanoconfined Bisphenol M Dicyanate Ester/Polycyanurate in Controlled Pore Glass. *Macromolecules* **2009**, *42*, 3573−3579.

(11) Koh, Y. P.; Li, Q. X.; Simon, S. L. T_g and Reactivity at the Nanoscale. *Thermochim. Acta* **2009**, *492*, 45−50.

(12) Koh, Y. P.; Simon, S. L. Trimerization of Monocyanate Ester in Nanopores. *J. Phys. Chem. B* **2010**, *114*, 7727−7734.

(13) Begum, F.; Simon, S. L. Modeling Methyl Methacrylate Free Radical Polymerization in Nanoporous Confinement. *Polymer* **2011**, *52*, 1539−1545.

(14) Zhao, H. Y.; Simon, S. L. Methyl Methacrylate Polymerization in Nanoporous Confinement. *Polymer* **2011**, *52*, 4093−4098.

(15) Begum, F.; Zhao, H. Y.; Simon, S. L. Modeling Methyl Methacrylate Free Radical Polymerization: Reaction in Hydrophilic Nanopores. *Polymer* **2012**, *53*, 3238−3244.

(16) Begum, F.; Zhao, H. Y.; Simon, S. L. Modeling Methyl Methacrylate Free Radical Polymerization: Reaction in Hydrophobic Nanopores. *Polymer* **2012**, *53*, 3261−3268.

(17) Ng, S. M.; Ogino, S.; Aida, T.; Koyano, K. A.; Tatsumi, T. Free Radical Polymerization within Mesoporous Zeolite Channels. *Macromol. Rapid Commun.* **1997**, *18*, 991−996.

(18) Kalogeras, I. M.; Neagu, E. R. Interplay of Surface And Confinement Effects on the Molecular Relaxation Dynamics of Nanoconfined Poly(methyl methacrylate) Chains. *Eur. Phys. J. E* **2004**, *14*, 193−204.

(19) Li, X. C.; King, T. A.; Pallikari-Viras, F. Characteristics of Composites Based on PMMA Modified Gel Silica Glasses. *J. Non-Cryst. Solids* **1994**, *170*, 243−249.

(20) Kageyama, K.; Ng, S. M.; Ichikawa, H.; Aida, T. Macromolecular Synthesis using Mesoporous Zeolites. *Macromol. Symp.* **2000**, *157*, 137−142.

(21) Uemura, T.; Ono, Y.; Kitagawa, K.; Kitagawa, S. Radical Polymerization of Vinyl Monomers in Porous Coordination Polymers: Nanochannel Size Effects on Reactivity, Molecular Weight, and Stereostructure. *Macromolecules* **2008**, *41*, 87−94.

(22) Ni, X. F.; Shen, Z. Q.; Yasuda, H. Polymerization of Methyl Methacrylate with Samarocene Complex Supported on Mesoporous Silica. *Chin. Chem. Lett.* **2001**, *12*, 821−822.

(23) Ikeda, K.; Kida, M.; Endo, K. Polymerization of Methyl Methacrylate with Radical Initiator Immobilized on the Inside Wall of Mesoporous Silica. *Polym. J.* **2009**, *41*, 672−678.

(24) Kalogeras, I. M.; Vassilikou-Dova, A. Dielectric Probe of Intermolecular Interactions in Poly(methyl methacrylate) (PMMA) and PMMA+SiO_2 Matrixes Doped with Luminescent Organics. *J. Phys. Chem. B* **2001**, *105*, 7651−7662.

(25) Pallikari-Viras, F.; Li, X. C.; King, T. A. Thermal Analysis of PMMA/Gel Silica Glass Composites. *J. Sol-Gel Sci. Technol.* **1996**, *7*, 203−209.

(26) Kalampounias, A. G.; Andrikopoulos, K. S.; Yannopoulos, S. N. "Rounding" of the Sulfur Living Polymerization Transition under Spatial Confinement. *J. Chem. Phys.* **2003**, *119*, 7543−7553.

(27) Andrikopoulos, K. S.; Kalampounias, A. G.; Yannopoulos, S. N. Confinement Effects on Liquid−Liquid Transitions: Pore Size Dependence of Sulfur's Living Polymerization. *Soft Matter* **2011**, *7*, 3404−3411.

(28) Tobolsky, A. V.; Eisenberg, A. Equilibrium Polymerization of Sulfur. *J. Am. Chem. Soc.* **1958**, *81*, 780−782.

(29) P. G. De Gennes *Scaling Concepts in Polymer Physics*; Cornell University Press: Ithaca, NY, 1979.

(30) Sakaue, T.; Raphael, E. Polymer Chains in Confined Spaces and Flow-Injection Problems: Some Remarks. *Macromolecules* **2006**, *39*, 2621−2628.

(31) Kong, C. Y.; Muthukumar, M. Polymer Translocation through a Nanopore. II. Excluded Volume Effect. *J. Chem. Phys.* **2004**, *120*, 3460−3466.

(32) Cacciuto, A.; Luijten, E. Self-Avoiding Flexible Polymers Under Spherical Confinement. *Nano Lett.* **2006**, *6*, 901−905.
(33) Smith, J. M.; Van Ness, H. C.; Abbott, M. M. *Introduction to Chemical Engineering Thermodynamics*; McGraw Hill: Boston, MA, 2005.
(34) Zheng, W.; Simon, S. L. Confinement Effects on the Glass Transition of Hydrogen Bonded Liquids. *J. Chem. Phys.* **2007**, *127*, 194501/1−11.
(35) Bryans, T. R.; Brawner, V. L.; Quitevis, E. L. Microstructure and Porosity of Silica Xerogel Monoliths Prepared by the Fast Sol-Gel Method. *J. Sol-Gel Sci. Technol.* **2000**, *17*, 211−217.
(36) Monine, M. I.; Posner, R. G.; Savage, P. B.; Faeder, J. R.; Hlavacek, W. S. Modeling Multivalent Ligand−Receptor Interactions with Steric Constraints on Configurations of Cell-Surface Receptor Aggregates. *Biophys. J.* **2010**, *98*, 48−56.
(37) Fairbrother, F.; Gee, G.; Merrall, G. T. The Polymerization of Sulfur. *J. Polym. Sci.* **1955**, *16*, 459−469.